

Ablative Rayleigh–Taylor instability with strong temperature dependence of the thermal conductivity

C. ALMARCHA¹, P. CLAVIN¹, L. DUCHEMIN¹ AND J. SANZ²

¹Institut de Recherche sur les Phénomènes Hors Equilibre, Universités d'Aix Marseille et CNRS, 49 rue Joliot Curie, BP 146, 13384 Marseille cedex 13, France

²ETSI Aeronauticos, Universidad Politecnica de Madrid, Madrid 28040, Spain

(Received 12 September 2006 and in revised form 21 December 2006)

An asymptotic analysis of Rayleigh–Taylor unstable ablation fronts encountered in inertial confinement fusion is performed in the case of a strong temperature dependence of the thermal conductivity. At leading order the nonlinear analysis leads to a free boundary problem which is an extension of the classical Rayleigh–Taylor instability with unity Atwood number and an additional potential flow of negligible density expelled perpendicular to the front. The nonlinear evolution of the front is analysed in two-dimensional geometry by a boundary integral method. The shape of the front develops a curvature singularity within a finite time, as for the Birkhoff–Rott equation for the Kelvin–Helmholtz instability.

1. Introduction

In inertial confinement fusion (ICF) the high fuel density which is required for nuclear burning can be obtained by imploding spherical shells by high-power laser radiation (direct drive). Irradiation leads to surface ablation and drives the capsule implosion. A layer of finite thickness (called the total thickness in the following) is formed between the ablation front in the cold (dense) material and the critical surface at low density and high temperature where the laser energy is deposited. The main mechanism of energy transfer between the laser deposition region and the cold material is thermal conduction. Owing to the temperature dependence of heat conductivity, the typical length scale of temperature variation increases strongly across the conduction region from d_a in the cold material to d_c at the critical surface (hot material), $d_a \ll d_c$. Such a scale separation is responsible for the existence of a thin ablation front with a large density jump separating the cold and dense material from the hot conduction region, see figure 1. Accelerating ablation fronts are Rayleigh–Taylor (RT) unstable while the short-wavelength disturbances are stabilized by ablation, see Bodner (1974). The self-consistent analyses of linear stability performed by Sanz (1994, 1996), Bychkov, Goldberg & Liberman (1994), Betti *et al.* (1995), and Goncharov *et al.* (1996) are too complicated to be extended into the nonlinear regime without further approximations. Nonlinear analyses have been performed by Sanz *et al.* (2002) and Clavin & Almarcha (2005) within the framework of a semi-empirical discontinuous model, called the sharp boundary model (SBM), consisting of two fluids of constant density separated by a front of zero thickness, see Betti, McCrory & Verdon (1993), Piriz, Sanz & Ibañez (1997), Piriz (2001) and Clavin & Masse (2004).

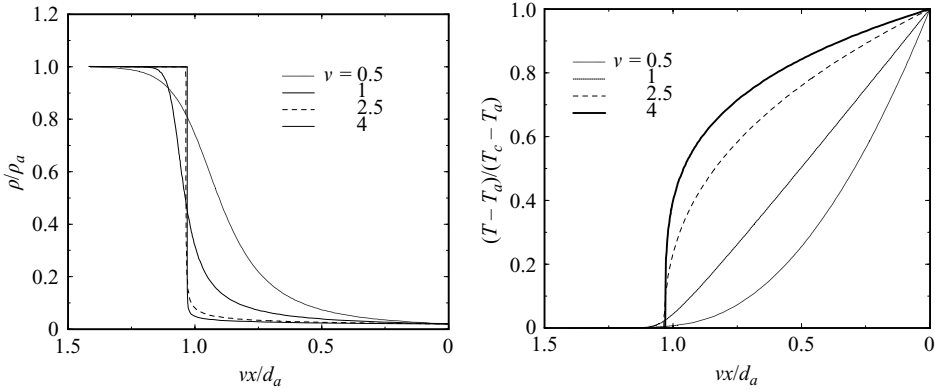


FIGURE 1. Density and temperature profiles for a Spitzer-type model with increasing ν and for $\Theta_c \equiv T_c/T_a = 50$.

The jump in density (across the ablation front) is a free parameter in the SBM, and an *ad hoc* assumption is required to close the problem. However, in the limit of an infinitely large density jump, the SBM leads to a simple formulation of the nonlinear problem that can be written in conveniently reduced variables as

$$\Delta\Psi_- = 0, \quad \Delta\Psi_+ = 0, \quad \lim_{\zeta \rightarrow -\infty} \Psi_- = 0, \quad \lim_{\zeta \rightarrow +\infty} \Psi_+ = \zeta, \quad (1.1a-d)$$

$$\mathbf{n} \cdot \nabla \Psi_-|_{\zeta=\zeta_f} = U_n^f, \quad \Psi_+|_{\zeta=\zeta_f} = 0, \quad \left[\frac{\partial \Psi_-}{\partial \tau} + \frac{|\nabla \Psi_-|^2}{2} + \frac{|\nabla \Psi_+|^2}{2} \right]_{\zeta=\zeta_f} = \zeta_f, \quad (1.2a-c)$$

where τ and $\boldsymbol{\zeta} = \zeta \mathbf{e}_x + \eta \mathbf{e}_y$ are reduced time and spatial coordinates, U_n^f is the normal velocity of the ablation front $\boldsymbol{\zeta}_f(t)$, and $\Psi_-(\boldsymbol{\zeta}, \tau)$ and $\Psi_+(\boldsymbol{\zeta}, \tau)$ are the velocity potentials of the cold and hot flow respectively. Except for the presence of Ψ_+ due to the hot flow expelled from the ablation front, the problem is like the RT problem with unity Atwood number. The uncontrolled approximations of the semi-empirical SBM limit the physical validity of the result, all the more so since the unknown density jump is used in the scaling of the reduced variables in (1.1) and (1.2), see Clavin & Almarcha (2005).

The objective of the present paper is twofold. First, by using an asymptotic analysis extending the linear study of Sanz, Masse & Clavin (2006) to the fully nonlinear regime, it is shown that the same equations as (1.1) and (1.2) are obtained from the basic equations for the conservation of mass, momentum and energy in a limit involving a strong temperature dependence of thermal conductivity, see (4.1) and (4.2). A major difference with the SBM is that the reduced variables appearing in (1.1) and (1.2) depend on the physical parameters defining the problem, namely the Froude number and the power index of thermal conductivity. Secondly, we obtain solutions in two-dimensional geometry of (1.1) and (1.2) by a boundary integral method in the spirit of the pioneering work of Baker, Meiron & Orszag (1980), as done by Duchemin, Josserand & Clavin (2005) in revisiting the RT instability. It is then shown that the front develops a curvature singularity within a finite time. The singularity is similar to the one observed in the solutions of the Birkhof–Rott equation describing the Kelvin–Helmholtz instability. The problem is formulated in § 2. The orders of magnitude are presented in § 3. The asymptotic analysis leading to (1.1) and (1.2) is developed in § 4. The nonlinear solution is presented in § 5.

2. Formulation

In the limit of a low Mach number and for a perfect gas, $\rho T = \rho_a T_a$, with a constant specific heat C_p , the fluid equations are

$$\partial_t \rho + \nabla \cdot (\rho \mathbf{u}) = 0, \quad (\partial_t + \mathbf{u} \cdot \nabla) \mathbf{u} = -\rho^{-1} \nabla p + g \mathbf{e}_x, \quad \nabla \cdot [\mathbf{u} - (\lambda / C_p \rho_a T_a) \nabla T] = 0. \quad (2.1a-c)$$

Here, ρ and T are the density and temperature respectively, p is the pressure, $\mathbf{u} = u \mathbf{e}_x + w \mathbf{e}_y$ is the flow velocity, x is the longitudinal coordinate and y is the transverse coordinates, \mathbf{e}_x and \mathbf{e}_y are the unit orthogonal vectors, \mathbf{e}_x pointing toward the hot material, λ is the heat conductivity, and g is the constant acceleration in the frame of the capsule. The upstream boundary condition are

$$x \rightarrow -\infty: \quad \rho = \rho_a, \quad T = T_a, \quad \mathbf{u} = V_a \mathbf{e}_x, \quad p = \bar{p}, \quad (2.2)$$

where V_a is the ablation velocity and \bar{p} the unperturbed pressure, $d(\bar{p} + \bar{\rho} \bar{u}^2)/dx = \bar{\rho} g$, the overline denoting unperturbed quantities. The laser intensity I , actually an energy flux, is absorbed at the critical density ρ_c , much lower than the initial density, $\rho_c \ll \rho_a$. In ICF, $\lambda(T) = \lambda_a \Theta^\nu$, $\Theta \equiv T/T_a$ denoting the reduced temperature. The power index is $\nu = 5/2$ for electron heat conduction and $\nu = 13/2$ for radiative heat conduction of a fully ionized plasma. Introducing the conduction length at the cold side, $d_a \equiv \lambda_a / \rho_a V_a$, three non-dimensional parameters characterize the problem: the inverse Froude number $Fr^{-1} \equiv g d_a / V_a^2$, the temperature ratio $\Theta_c \equiv T_c / T_a = \rho_a / \rho_c \gg 1$ and the power index ν . The conduction length at the critical surface is $d_c \equiv d_a \Theta_c^\nu$ and d_c / ν is the total thickness of the thermal wave. In conditions of ICF implosion, $\Theta_c \gg 1$ and the acceleration is such that $1 / \Theta_c^{\nu-1} \ll Fr^{-1} / \nu < 1$. Therefore, the wavelengths of the most unstable disturbance and of the marginal mode (zero linear growth rate) are of the same order of magnitude $2\pi / k_m$ such that $\nu / d_c \ll k_m \ll 1 / d_a$. The thermal perturbations cannot reach the critical surface which remains planar. The downstream boundary conditions then reduce to

$$x \rightarrow +\infty: \quad T - \bar{T} = 0, \quad \mathbf{u} \quad \text{and} \quad p - \bar{p} \quad \text{bounded}. \quad (2.3)$$

Equations (2.1) to (2.3) constitute the basic framework for studying the ablation front during the implosion in ICF, see Atzeni & Meyer-Ter-Vehn (2004). The unperturbed temperature profile upstream of the critical surface is a solution to the first-order equation $\bar{\mu} C_p (\bar{T} - T_a) - \lambda d\bar{T}/dx = 0$ where $\bar{\mu}$ denotes the unperturbed ablation rate, $\bar{\mu} \equiv \rho_a V_a = I / C_p (T_c - T_a)$. At the cold side, the profile of temperature (or density) presents a sharp bend of width of order d_a , representative of the ablation front, see figure 1. Choosing the origin of the x -axis at the bend, the temperature profile satisfies a power law in the hot region where terms of order $1/\bar{\Theta}$ are negligible,

$$\bar{\Theta} \equiv \bar{T}(x) / T_a \approx (\nu x / d_a)^{1/\nu}, \quad \bar{\theta}(x) \equiv \bar{\Theta}^\nu(x) / \nu \approx x / d_a. \quad (2.4)$$

This outer solution is singular at the origin where the ablation front is located. Focusing attention on intermediate wavelengths, $\nu / d_c \ll k \ll 1 / d_a$, equations (2.1) to (2.3) describe a free boundary problem with two external regions: a constant-density region of dense and cold medium (subscript $-$), $\rho_- = \rho_a$, $\Theta = 1$, and a hot conduction region (subscript $+$), $\Theta \equiv T / T_a = \rho_a / \rho_+ \gg 1$, separated by a thin ablation front located at $x = \alpha(y, t)$ (to simplify notation the Cartesian equation of the front is written for a single-valued surface, but the method applies for a multi-valued front). Density and temperature vary in the hot region.

Let us split the flow within the hot side into two parts, $\mathbf{u}_+ = \mathbf{u}_+^{(p)} + \mathbf{u}_+^{(r)}$, where $\mathbf{u}_+^{(p)} \equiv V_a d_a \Theta \nabla \theta$ is associated with the thermal flux $\Theta^\nu \nabla \Theta = \Theta \nabla \theta$, $\theta \equiv \Theta^\nu / \nu$. According to

(2.1), $\nabla \cdot \mathbf{u}_+^{(r)} = 0$, and the thermal equation yields

$$(\partial_t + \mathbf{u}_+^{(r)} \cdot \nabla) \Theta^{-1} + V_a d_a \Delta \theta = 0, \quad \theta \equiv \Theta^v / \nu, \quad \mathbf{u}_+ = \mathbf{u}_+^{(p)} + \mathbf{u}_+^{(r)}, \quad \mathbf{u}_+^{(p)} \equiv V_a d_a \Theta \nabla \theta. \quad (2.5)$$

In the limit $kd_a \rightarrow 0$, equations (2.1) lead to jumps in density, temperature Θ_{f+} , mass flux and pressure across the ablation front while conservation of energy gives the mass flux in terms of the local gradient of temperature,

$$[\rho(\mathbf{u} \cdot \mathbf{n} - u_n^f)]_{x=\alpha_-}^{x=\alpha_+} = 0, \quad [(\mu_f^2/\rho) + p]_{x=\alpha_-}^{x=\alpha_+} = 0, \quad \mathbf{u}^{(r)}|_{x=\alpha_+} = \mathbf{u}_-|_{x=\alpha_-}, \quad (2.6a-c)$$

$$\mu_f / \rho_a V_a = (1 - 1/\Theta_{f+}) d_a \mathbf{n} \cdot \nabla \theta|_{x=\alpha_+} \approx d_a \mathbf{n} \cdot \nabla \theta|_{x=\alpha_+}, \quad (2.7a, b)$$

where $x = \alpha_+$ and $x = \alpha_-$ denote the hot and cold side respectively, \mathbf{n} is the unit vector perpendicular to the front (pointing in the direction of the hot side), $u_n^f \equiv [1 + (\partial\alpha/\partial y)^2]^{-1/2} \partial\alpha/\partial t$ is the normal velocity of the front in the frame of the unperturbed front, and μ_f is the ablation rate (mass flux across the ablation front, $\mu_f \equiv \rho(\mathbf{u} \cdot \mathbf{n} - u_{nf})|_{x=\alpha}$). Equation (2.6c) comes from the conservation of the tangential component of the flow velocity together with equation (2.1c) and the definition of $\mathbf{u}^{(p)}|_{x=\alpha_+}$.

3. Orders of magnitude

We consider intermediate accelerations, $1/\Theta_c^{v-1} \ll Fr^{-1}/\nu \ll 1$ in two-dimensional geometry. An asymptotic analysis is then performed using the small parameter $\varepsilon \equiv (Fr^{-1}/\nu)^{1/(2(v-1))}$. At leading order in the distinguished limit $\varepsilon \rightarrow 0$, $\Theta_c \rightarrow \infty$, $\varepsilon \Theta_c^{1/2} \rightarrow \infty$, consistent with the real conditions, the linear growth rate σ of a perturbation of wavelength $2\pi/k$ is

$$\sigma d_a / V_a = \sqrt{(kd_a) Fr^{-1} - (kd_a)^{2-1/\nu} q_o^* \nu^{1/\nu}}, \quad S = \sqrt{K - q_o^* K^{2-1/\nu}} \quad (3.1a, b)$$

where $S > 0$, $K > 0$ and $q_o^* = d^2 \tilde{\varphi}_o / d\xi^2|_{\xi=0}$ are quantities of order unity,

$$K \equiv kd_a / \nu \varepsilon^{2\nu} = O(1), \quad S \equiv (\sigma d_a / V_a) / \nu \varepsilon^{2\nu-1} = O(1), \quad (3.2a, b)$$

with $\tilde{\varphi}_o(\xi)$ the solution to the fifth-order system describing the hot conduction region ($\xi \geq 0$),

$$\frac{d^3 \tilde{\varphi}_o}{d\xi^3} - \frac{d\tilde{\varphi}_o}{d\xi} - \frac{\tilde{\varphi}_o}{\nu \xi} = -\frac{d\tilde{\theta}_o/d\xi}{\nu \xi^{1-1/\nu}}, \quad \frac{d^2 \tilde{\theta}_o}{d\xi^2} - (\tilde{\theta}_o - 1) = -\frac{\tilde{\varphi}_o}{\nu \xi^{1+1/\nu}} \quad (3.3a, b)$$

and satisfying to the five boundary conditions

$$\xi = 0 : \tilde{\varphi}_o = 0, \quad d\tilde{\varphi}_o/d\xi = 0, \quad \tilde{\theta}_o = 0; \quad \xi \rightarrow +\infty : d\tilde{\varphi}_o/d\xi = 0, \quad \tilde{\theta}_o = 1, \quad (3.4)$$

where $\xi \equiv k(x - \alpha)$, see Sanz *et al.* (2006). Equation (3.3b) is the heat transfer equation (2.5), and $\tilde{\theta}_o$ is related to the perturbation $\delta\theta$, $\theta = \bar{\theta}(x - \alpha) + \delta\theta$, while $\tilde{\varphi}_o$ represents the stream function of the solenoidal flow $\mathbf{u}_+^{(r)}$. More precisely, for a perturbed front of the form $\alpha/d_a = \bar{\alpha} e^{iky + \sigma t}$, $\tilde{\theta}_o$ and $\tilde{\varphi}_o$ are defined by $\delta\theta_o = \tilde{\theta}_o \bar{\alpha} e^{iky + \sigma t}$ and $\varphi_o = \tilde{\varphi}_o \bar{\alpha} e^{iky + \sigma t}$, the subscript o denoting the leading order. Introducing $\delta\mathbf{u}_+^{(r)}$, $\mathbf{u}_+^{(r)} = V_a + \delta\mathbf{u}_+^{(r)}$, the components of $(kd_a)^{-1+1/\nu} \nu^{-1/\nu} \delta\mathbf{u}_+^{(r)} / V_a$ are $(-\varphi_o, -id\varphi_o/d\xi)$. Pressure and vorticity $\nabla \times \delta\mathbf{u}_+^{(r)}$ are represented by $d^2 \tilde{\varphi}_o / d\xi^2 - d(\xi^{1/n} \tilde{\theta}_o) / d\xi$ and $\tilde{\varphi}_o - d^2 \tilde{\varphi}_o / d\xi^2$ respectively.

Let us now consider the orders of magnitude. According to (3.3) and (3.4), $\tilde{\theta}_o$ is of order unity, $\delta\theta_o(\xi) = O(\alpha/d_a)$. The perturbed ablation rate $\delta\mu_f$ is evaluated from its definition (2.7) with $\nabla\delta\theta = O(k\delta\theta)$, $\delta\mu_f/\bar{\mu} = O(k\alpha)$. The order of magnitude $\delta\mathbf{u}_+^{(r)}/V_a = O(\varepsilon^{-2}k\alpha\tilde{\varphi}_o)$ is obtained from the expression of $\delta\mathbf{u}_+^{(r)}/V_a$ in terms of φ_o by using $(kd_a/\nu)^{1/\nu} = O(\varepsilon^2)$, see (3.2). Downstream of the ablation front, in the region where $\xi = O(1)$, the unperturbed temperature $\bar{\Theta}(\xi)$ is, according to $(kd_a/\nu)^{-1/\nu} = O(\varepsilon^{-2})$, of order $1/\varepsilon^2$, see (2.4). The order of magnitude $\delta\mathbf{u}_+^{(p)}/V_a = O(\varepsilon^{-2}k\alpha)$ is obtained from the definition $\mathbf{u}_+^{(p)} \equiv V_a d_a \Theta \nabla\theta$ with $\nabla\delta\theta = O(k\delta\theta)$. In the hot conduction region a quasi-steady approximation applies because $\bar{\rho}_+ \partial_t = O(\varepsilon\rho_a V_a \partial_x)$, as a consequence of (3.2), $\sigma/V_a k = O(\varepsilon^{-1})$, together with $\bar{\rho}_+/\rho_a = 1/\Theta_+ = O(\varepsilon^2)$. The pressure is evaluated from $\rho_a V_a \partial_x \delta u_+ \approx -\partial_x \delta p_+$, and the orders of magnitude in the hot side are

$$\delta\theta_o(\xi) = O(\alpha/d_a), \quad \delta\mu_f/\bar{\mu} = O(k\alpha), \quad \delta\mathbf{u}_+^{(p)}/V_a = O(\varepsilon^{-2}k\alpha), \quad (3.5)$$

$$\delta p_+(\xi)/\rho_a V_a^2 = O(\varepsilon^{-2}k\alpha), \quad \delta\mathbf{u}_+^{(r)}/V_a = O(\varepsilon^{-2}k\alpha\tilde{\varphi}_o). \quad (3.6)$$

In the cold region upstream of the ablation front where the density is constant, the pressure is evaluated from (2.1) by using $\sigma/V_a k = O(\varepsilon^{-1})$, $\partial_x \delta u_- \sim k\delta u_-$, $\partial_x \delta p_- \sim k\delta p_-$, so that $\rho_a \sigma \delta u_- \sim -k\delta p_-$, and $\delta u_-/V_a = O(\varepsilon\delta p_-/\rho_a V_a^2)$. The order of magnitude of the pressure being the same on both sides of the ablation front, the perturbed flow velocity in the cold side is smaller than in the hot conduction region by a factor ε , but larger than the ablation velocity by a factor $1/\varepsilon$:

$$\delta p_-/\rho_a V_a^2 = O(\varepsilon^{-2}k\alpha), \quad \delta\mathbf{u}_-/V_a = O(\varepsilon^{-1}k\alpha), \quad \delta u_{nf} - |\delta\mathbf{u}_-|_{\xi=0} = O(\varepsilon|\delta\mathbf{u}_-|_{\xi=0}). \quad (3.7)$$

4. Nonlinear analysis

In the limit we consider from now on, $\nu \gg 1$, the last term on the left-hand side of equation (3.3a) together with the right-hand side of (3.3b) become negligible so that θ is a solution of Laplace equation. An explicit solution of (3.4) is

$$d\tilde{\varphi}_o/d\xi = -e^{-\xi} \int_0^\infty x^{1/\nu} e^{-2x} dx + e^\xi \int_\xi^\infty x^{1/\nu} e^{-2x} dx,$$

showing that $\tilde{\varphi}_o$ and $d\tilde{\varphi}_o/d\xi$ are of order $1/\nu$, $\delta\mathbf{u}_+^{(r)} = O(\delta\mathbf{u}_+^{(p)}/\nu)$ see (3.5), (3.6). This also indicates the existence of a boundary layer at $\xi = 0$ where the vorticity $\nabla \times \delta\mathbf{u}^{(r)}$ is localized, $\xi \ll 1$: $d\tilde{\varphi}_o/d\xi \approx \xi(1 - \xi^{1/\nu})$, $d^2\tilde{\varphi}_o/d\xi^2 \approx 1 - \xi^{1/\nu}$; $\xi = O(1)$: $d^2\tilde{\varphi}_o/d\xi^2 = O(1/\nu)$. This suggests performing the nonlinear analysis in the distinguished limits

$$\nu \rightarrow \infty, \quad \varepsilon^2 \equiv (Fr^{-1}/\nu)^{1/(\nu-1)} \rightarrow 0, \quad \Theta_c \equiv \rho_a/\rho_c \rightarrow \infty, \quad \varepsilon^2 \Theta_c \rightarrow \infty, \quad (4.1)$$

for amplitudes of the wrinkled front of same order as the wavelength,

$$\alpha k = O(1), \quad \alpha/d_a = O(\varepsilon^{-2\nu} \nu^{-1}), \quad (4.2)$$

see (3.2). The parameter Θ_c will no longer appear in the rest of the analysis, since the last two conditions in (4.1) are there only to ensure the validity of (2.3), $k_m d_c/\nu \gg 1$, while $\varepsilon \rightarrow 0$ ensures $k_m d_a \ll 1$, see Sanz *et al.* (2006).

Considering length and time scales of the order of the most linearly amplified wavelength and its linear growth, the useful non-dimensional variables are, according to (3.2),

$$\zeta = (\mathbf{r}/d_a)\varepsilon^2 Fr^{-1}, \quad \tau = (tV_a/d_a)\varepsilon Fr^{-1} \quad \text{with} \quad \varepsilon^2 Fr^{-1} = \nu\varepsilon^{2\nu}, \quad (4.3)$$

see (4.1). In the system of coordinates, $\zeta = (\zeta, \eta)$, ζ and η denote the longitudinal and transverse coordinates respectively, and the coordinates of the ablation front

will be denoted by ζ_f . The orders of magnitude of the fully nonlinear regime are obtained by introducing (4.2) into (3.5), (3.6) and (3.7) after using (3.2). Hence the non-dimensional quantities of order unity in the limit (4.1) for characterizing the ablation rate $\Delta\mu \equiv \mu - \bar{\mu}$, the normal velocity of the front u_n^f and the flow $\Delta\mathbf{u}_\pm \equiv \mathbf{u}_\pm - \bar{\mathbf{u}}_\pm$, $\Delta\pi_\pm \equiv \pi_\pm - \bar{\pi}_\pm$ with $\pi_\pm \equiv p_\pm - \rho_\pm g x$ are $M(\zeta_f, \tau)$, $U_n^f(\zeta_f, \tau)$, $\mathbf{U}_\pm(\zeta, \tau)$, $\Pi_\pm(\zeta, \tau)$, defined as follows:

$$\Delta\mu/\bar{\mu} \equiv M, \quad u_n^f/V_a \equiv U_n^f/\varepsilon, \quad (4.4a, b)$$

$$\Delta\mathbf{u}_-/V_a \equiv \mathbf{U}_-/ \varepsilon, \quad \Delta\pi_-/\rho_a V_a^2 \equiv \Pi_-/\varepsilon^2, \quad \Delta\mathbf{u}_+/V_a \equiv \mathbf{U}_+/\varepsilon^2, \quad \Delta\pi_+/\rho_a V_a^2 \equiv \Pi_+/\varepsilon^2. \quad (4.5)$$

Equation (4.4b) is obtained from (3.2), $\sigma/V_a k = O(1/\varepsilon)$, $\partial\alpha/\partial t = O(\sigma/k)$.

Let us now show that a constant-density approximation holds at leading order downstream of the front. According to (2.4) and (3.2a), one has $\bar{\Theta} = (\xi/K)^{1/\nu} \varepsilon^{-2}$, with, according to (3.5) and (4.2), $\delta\theta = O(\varepsilon^{-2\nu}/\nu)$. The perturbations of θ , p and \mathbf{u}_+^p decreasing to zero exponentially fast with increasing ξ , the perturbation of ρ vanishes outside the region $\xi = O(1)$ where $\bar{\rho}$ is constant and $\delta\rho$ is smaller than $\bar{\rho}$ at leading order in the limit (4.1),

$$\xi = O(1): \quad \bar{\rho}_{o+}(\xi)/\rho_a = 1/\bar{\Theta}_o = \varepsilon^2, \quad \delta\rho_{o+}(\xi)/\rho_a = -\delta\theta_o/\bar{\Theta}_o^{v+1} = O(\varepsilon^2/\nu). \quad (4.6)$$

In addition, according to the comment above (4.1), the flow is potential in this region, $\mathbf{u}_{o+} = \mathbf{u}_{o+}^{(p)} = V_a d_a \nabla\theta_o/\varepsilon^2$.

The vicinity of the origin $\xi = 0$ is more tricky, and requires special attention. The boundary conditions (3.4) at $\xi = 0$ together with the expression $q_o^* = d^2\tilde{\varphi}_o/d\xi^2|_{\xi=0}$ are obtained from (2.6) and (2.7) for a matching region on the hot side of the ablation front corresponding to $\bar{\Theta} = O(1/\varepsilon)$. There, the variation of the dynamical pressure $\delta(\mu_f^2/\rho)$ is smaller than δp by a factor ε , so that relation (2.6b) is $[\delta p_o]_\pm^+ = 0$. Not only is the vorticity localized inside the boundary layer $1/\varepsilon \leq \Theta < 1/\varepsilon^2$, but also the variations of dynamical pressure are of order $1/\varepsilon$ in this layer, while the variation of pressure is of order unity. However the thickness (measured with the ξ -variable) of the layer shrinks to zero in the limit $\nu \rightarrow \infty$. Therefore the analysis may be carried out in the limit (4.1) by incorporating the layer $\varepsilon \geq \rho_+/ \rho_a > \varepsilon^2$ into the ablation front where μ_f^2/ρ must be retained in the jump in pressure. The ablation front becomes a vortex sheet, separating two regions of constant density $\rho_- = \rho_a$, $\rho_+ = \varepsilon^2 \rho_a$ where the flow is in irrotational motion.

The space variables ξ and ζ being obtained from the original space variable x/d_a with the same scaling, see (3.2) and (4.3), the leading-order Euler equations can then be written in non-dimensional form

$$\partial\mathbf{U}_-/\partial\tau + (\mathbf{U}_- \cdot \tilde{\nabla})\mathbf{U}_- = -\tilde{\nabla}\Pi_-, \quad \partial\mathbf{U}_+/\partial\zeta + (\mathbf{U}_+ \cdot \tilde{\nabla})\mathbf{U}_+ = -\tilde{\nabla}\Pi_+, \quad (4.7)$$

with $\tilde{\nabla} \cdot \mathbf{U}_- = 0$ and $\tilde{\nabla} \cdot \mathbf{U}_+ = 0$, $\tilde{\nabla}$ denoting the gradient with respect to ζ . Here, the approximation of a negligible unperturbed velocity in the cold flow, $V_a/u_- = O(\varepsilon)$ see (4.5), and a steady-state approximation in the hot flow, $\partial_t = O(\varepsilon \bar{u}_+ \partial_x)$, has been used.

Let us now go back to the jump conditions across the front. According to (4.4) and (4.5), $u_n^f = O(|\mathbf{u}_-|)$, $|\mathbf{u}_-| = O(V_a/\varepsilon)$, the normal velocity of the ablation front is larger than the ablation velocity V_a , but smaller than the perturbed velocity of the expelled hot fluid, $|\mathbf{u}_-| = O(\varepsilon|\mathbf{u}_+|)$. Mass conservation, equation (2.6a), then leads to

$$\mathbf{n} \cdot \mathbf{U}_-|_{\zeta=\zeta_f} = U_n^f, \quad \mathbf{n} \cdot (\mathbf{e}_x + \mathbf{U}_+)|_{\zeta=\zeta_f} = 1 + M, \quad (4.8a, b)$$

where U_n^f is the velocity normal to the front $\xi_f(t)$ in the system of coordinates (4.3). Equation (4.8a) expresses that the front moves with the cold fluid, and (4.8b) that the flow velocity of the hot flow is controlled by the ablation rate only. In other words, the ablation rate is negligible in the cold side, $|\mathbf{u}_-|/V_a = O(1/\varepsilon)$ and $\mu/\bar{\mu} = O(1)$, while the front velocity is negligible in front of the flow velocity in the hot fluid, $u_n^f = O(\varepsilon|\mathbf{u}_+|)$. By using (2.4), $d_a \mathbf{n} \cdot \nabla \bar{\theta}|_{\zeta=\xi_f} = \mathbf{n} \cdot \mathbf{e}_x$, equation (4.8b) together with equation (2.7a) leads to $\mathbf{n} \cdot \mathbf{U}_+|_{\zeta=\xi_f} = d_a \mathbf{n} \cdot \nabla(\theta - \bar{\theta})|_{\zeta=\xi_f}$. This can be written in terms of a velocity potential Φ_+ of order unity, $\mathbf{n} \cdot \mathbf{U}_+|_{\zeta=\xi_f} = \mathbf{n} \cdot \tilde{\nabla} \Phi_+|_{\zeta=\xi_f}$, where by definition $\Phi_+ \equiv (\theta - \bar{\theta})Fr^{-1} = O(1)$, see (4.3) and (4.6). According to the leading order of (2.4) and (2.5), $\Delta \bar{\theta} = 0$, $\Delta \theta = 0$, and the velocity potential Φ_+ is a solution to Laplace equation. On the other hand, the hot fluid velocity being larger than the cold fluid velocity, $|\mathbf{u}_+| = O(|\mathbf{u}_-|/\varepsilon)$, conservation of transverse momentum implies that the hot fluid is expelled quasi-perpendicularly to the front, $\mathbf{t} \cdot (\mathbf{e}_x + \mathbf{U}_+)|_{\zeta=\xi_f} = 0$, where \mathbf{t} is the unitary vector tangent to the front. Viewed from the hot side, the front is an isotherm, $\mathbf{t} \cdot \nabla \theta|_{\zeta=\xi_f} = 0$ equivalent to $\mathbf{t} \cdot (\mathbf{e}_x + \tilde{\nabla} \Phi_+)|_{\zeta=\xi_f} = 0$, so that $\mathbf{t} \cdot \mathbf{U}_+|_{\zeta=\xi_f} = \mathbf{t} \cdot \tilde{\nabla} \Phi_+|_{\zeta=\xi_f}$. Hence the boundary condition of the hot flow is $\mathbf{U}_+|_{\zeta=\xi_f} = \tilde{\nabla} \Phi_+|_{\zeta=\xi_f}$. This is in full agreement with an incompressible and a potential flow and slaved to the temperature, as in the linear approximation, $\mathbf{U}_+ = \tilde{\nabla} \Phi_+$.

The flows \mathbf{U}_- and \mathbf{U}_+ being irrotational, (4.7) can be written as $\partial \mathbf{U}_-/\partial \tau = -\tilde{\nabla}\{\Pi_- + |\mathbf{U}_-|^2/2\}$ and $\partial \mathbf{U}_+/\partial \zeta = -\tilde{\nabla}\{\Pi_+ + |\mathbf{U}_+|^2/2\}$, giving

$$\partial \Psi_-/\partial \tau = -\Pi_- - |\tilde{\nabla} \Psi_-|^2/2, \quad \partial \Phi_+/\partial \zeta = -\Pi_+ - |\tilde{\nabla} \Phi_+|^2/2, \quad (4.9)$$

where Ψ_- is the velocity potential of the cold flow, $\mathbf{U}_- = \tilde{\nabla} \Psi_-$, with $\lim_{\zeta \rightarrow -\infty} \Psi_- = 0$ and $\mathbf{n} \cdot \tilde{\nabla} \Psi_-|_{\zeta=\xi_f} = U_n^f$, see (4.8). According to (2.3) and (2.4), the boundary conditions for Φ_+ are $\lim_{\zeta \rightarrow +\infty} \Phi_+ = 0$ and $\Phi_+|_{\zeta=\xi_f} = -\zeta_f$. The dynamics of the ablation front $\zeta_f(\tau)$ is then obtained by solving two Laplace equations, $\Delta \Psi_- = 0$ and $\Delta \Phi_+ = 0$, with the four boundary conditions just mentioned above, plus a fifth one at the front for conservation of longitudinal momentum, obtained from equation (2.6b),

$$[\pi_- - \pi_+]_{x=\alpha} = (1 + M)^2/\varepsilon^2 - (\alpha/d_a)Fr^{-1}. \quad (4.10)$$

The first term on the right-hand side is the dynamical pressure and the second is the acceleration. According to (4.1), (4.2) and (4.3), $(\alpha/d_a)Fr^{-1} = \zeta_f/\varepsilon^2$, so that the three terms in (4.10) are of same order, see (4.5) and the discussion after (4.6) concerning the vicinity of $\xi = 0$. Therefore, according to equation (4.8b) together with (4.9), the conservation of longitudinal momentum across the front takes the following non-dimensional form:

$$\left[\frac{\partial \Psi_-}{\partial \tau} - \frac{\partial \Phi_+}{\partial \zeta} + \frac{|\tilde{\nabla} \Psi_-|^2}{2} - \frac{|\tilde{\nabla} \Phi_+|^2}{2} \right]_{\zeta=\xi_f} = 1 - [\mathbf{n} \cdot (\mathbf{e}_x + \tilde{\nabla} \Phi_+)|_{\zeta=\xi_f}]^2 + \zeta_f. \quad (4.11)$$

This equation is similar to that obtained in the semi-empirical SBM of Clavin & Almarcha (2005) for $Fr^{-1} = O(1)$ in the limit of a large jump in density across the ablation front. According to the present analysis, equation (4.11) is obtained in a systematic way in the limit (4.1). Moreover, according to (4.6), the unknown jump in density appearing in the scalings of the SBM is now determined: $\rho_+/\rho_a = (Fr^{-1}/\nu)^{1/(v-1)}$. Recalling that constant terms are irrelevant and that the hot flow is orthogonal to the ablation front, the right hand side of (4.11) may be written in a simpler form

$$|\mathbf{n} \cdot (\mathbf{e}_x + \tilde{\nabla} \Phi_+)|_{\zeta=\xi_f} = |\mathbf{e}_x + \tilde{\nabla} \Phi_+|_{\zeta=\xi_f}$$

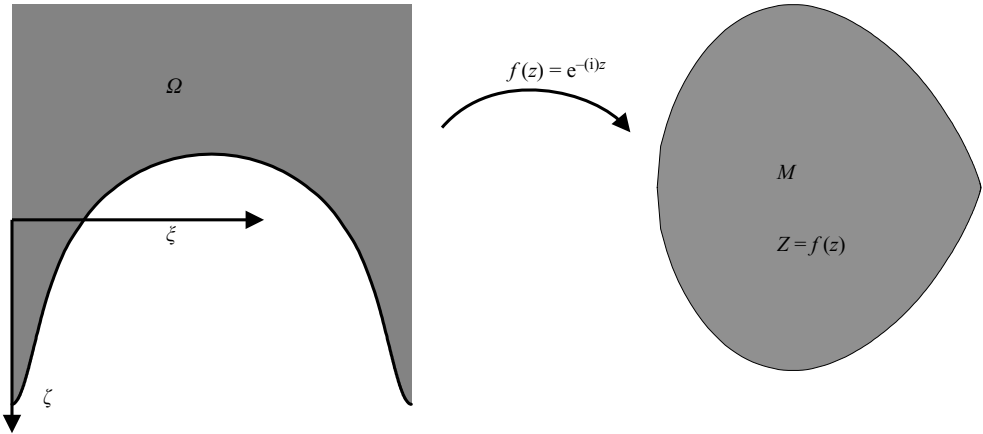


FIGURE 2. Conformal map used to transform the periodic surface into a bounded domain.

Considering infinitesimal disturbances in the form $e^{S\tau \pm iK\eta}$, the linear analysis leads to the linear growth rate $S = \sqrt{K - K^2}$, in full agreement with (3.1), since the solution to (3.3) and (3.4) shows that $\lim_{v \rightarrow +\infty} [d^2 \tilde{\varphi}_o / d\xi^2 |_{\xi=0}] = 1$, see Sanz *et al.* (2006). When the velocity potential of the total flow $\Psi_+ \equiv \Phi_+ + \zeta$ is introduced into (4.11), the free boundary problem takes the simpler form (1.1), (1.2) describing an extension of the RT problem for an inviscid fluid above a vacuum without surface tension. The numerical solution of this problem is discussed in the next section.

5. Results and discussion

Accurate numerical solutions to (1.1) and (1.2) are obtained in periodic two-dimensional geometry with an extension of the boundary integral method of Duchemin *et al.* (2005). We first briefly explain the method. Thanks to the potential flow approximation, all the useful information is concentrated on the interface. The power of boundary integral methods consists of reducing the dimension of the problem by one: from two dimensions to one dimension in our case. The method utilizes a highly non-uniform set of collocation points placed on the front and redistributed at each time-step in order to ensure a good accuracy in regions where the curvature of the front is large. Particular attention is paid to the redistribution in order to be sure that it does not introduce spurious effects. At each time-step, knowing Ψ_- and $\Phi_+ = \Psi_+ - \zeta$ on the front (i.e. on the collocation points), the Laplace equation is solved to find the velocities of the fluid particles on each side of the front. This computation is performed using the conformal map $Z = e^{-iz}$, $z = \xi + i\zeta$, to transform the periodic domain into a bounded domain where the Cauchy theorem applies, see figure 2. The discrete version of the Cauchy theorem gives us the streamfunctions corresponding respectively to Ψ_- on the cold side and Φ_+ on the hot side. Knowing the streamfunctions and the velocity potentials on each side, we deduce the normal and tangential gradients of Ψ_- and Φ_+ . The points on the front are advected using (1.2a) while the velocity potential Ψ_- is updated using the boundary condition (1.2c), after introducing the material derivative $\partial \Psi_- / \partial \tau + |\nabla \Psi_-|^2 / 2$. Finally the time-stepping method used to obtain the evolution of the front pattern is a fourth-order Runge–Kutta scheme with a time-step decreasing according to the minimum arclength between two successive points on the surface.

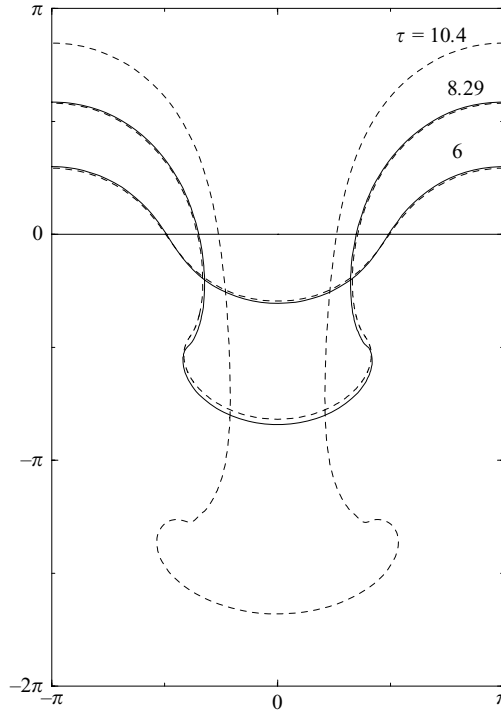


FIGURE 3. Numerical solution of (1.1), (1.2) (solid line) at various times for a sinusoidal disturbance with the wavelength of the most linearly amplified mode, initial amplitude: 0.1. The curvature singularity is spontaneously formed at $\tau = 8.29$. A smooth solution (dashed line) is obtained when a small surface-tension-like term, 0.004 curvature, is added from the beginning in (1.2c).

An example of solution is shown in figure 3. Unlike the RT instability with unity Atwood number ($A = 1$) and zero surface tension, the problem does not possess a smooth solution for more than a finite time, as for the solution of the Birkhoff–Rott equation studied by Moore (1979) and also for the RT instability with $A < 1$, see Baker, Caflich & Siegel (1993) and Matsuoka & Nishihara (2006). The shape of the front develops a singularity within a finite time, the inclination of the tangent to the front stays finite and a continuous but infinite curvature develops. The points of maximum and minimum curvature (of opposite sign on both sides of the zero curvature point) collapse in finite time, while the absolute value of the curvature blows up. Using the boundary integral method, we were able to approach the singularity with great accuracy. Figure 4 shows the time evolution of the following quantities: the derivative of the curvature with respect to the arclength s at the inflection point $\kappa'(s)$, the maximum and minimum curvatures around the inflection point κ_{max} and κ_{min} and the distance in arclength between these last two points $s_{max} - s_{min}$. The critical time τ_0 at which the singularity develops is found by requiring that the behaviour of these quantities in powers of $\tau_0 - \tau$ is observed for a large number of decades. A remarkable behaviour in powers of $\tau_0 - \tau$ is observed independently of the wavenumber. The scaling laws derived from numerical fitting in figure 4 are self-consistent since a variation of the curvature $(\tau_0 - \tau)^{-1}$ on an arclength distance $(\tau_0 - \tau)^{4/3}$ gives a curvature derivative in $(\tau_0 - \tau)^{-7/3}$. The exponents are accurate within a few percent. Figure 5 shows the rescaled curvature as a function of the rescaled arclength for

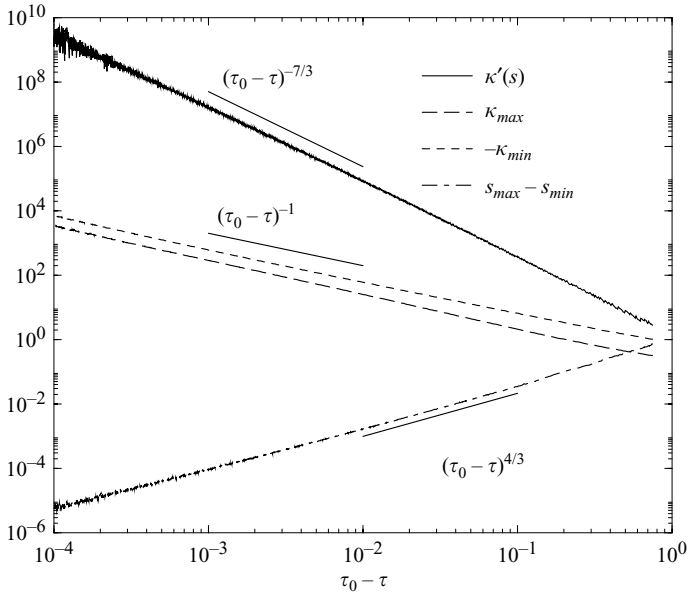


FIGURE 4. $\kappa'(s)$, κ_{max} , $-\kappa_{min}$ and $s_{max} - s_{min}$ as a function of $\tau_0 - \tau$ in a log-log plot.

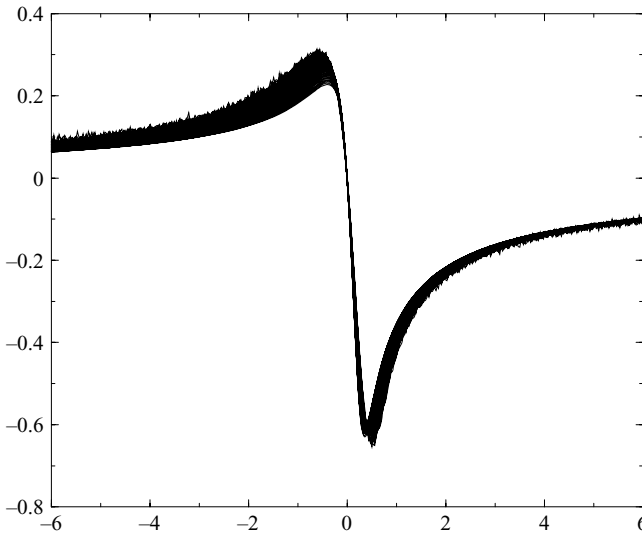


FIGURE 5. Rescaled curvature according to $(\tau_0 - \tau)^{-1}$ as a function of the arclength rescaled according to $(\tau_0 - \tau)^{4/3}$.

various time-steps. The very good collapse of these curves exhibits a self-similarity solution of the problem close to the critical time τ_0 .

The nonlinearity introduced by ablation $|\tilde{\nabla}\Phi_+|^2$ plays a key role in the singularity formation, since such a singularity is not observed in the RT problem with $A = 1$ for which Φ_+ does not exist, see Duchemin *et al.* (2005). There is however an indication that the singularity is smoothed out at following orders of the asymptotic expansion when the finite thickness of the ablation front is taken into account. If a small

surface-tension-like term is introduced into the right-hand side of (1.2c) for modelling the finite thickness effect of the curved front, as for wrinkled flames, see Pelcé & Clavin (1982), the arclength between the extrema of curvature still decreases to zero but in infinite time, exponentially, while the curvature modulus increases exponentially. The rest of the front shape is not influenced sensitively by the small surface-tension-like effect. For periodic conditions and infinitesimal initial disturbances, the tip of the bubble reaches the same constant curvature and velocity in the long time limit as in the RT problem investigated by Taylor (1950), but with an overshoot. This is confirmed by a local analysis with a single-mode approximation of the Layzer-type, see Layzer (1955), but with a different wavenumber for Ψ_- and Ψ_+ , showing that the contribution of $|\nabla\Psi_+|^2$ in (1.2) gives a constant term in the long time limit. The spike continues to accelerate while its radius increases with time, unlike the radius of curvature of the RT spike which decreases in time like $1/\tau^3$, see Clavin & Williams (2005) and Duchemin *et al.* (2005).

To conclude, the free boundary problem (1.1), (1.2) is mathematically ill-posed for general classes of initial conditions, since a curvature singularity appears within a finite time, but it provides a simple and useful framework for studying the nonlinear growth of the hydrodynamical instability of ablation fronts in ICF, at least before the sudden formation of the singularity. With our regularizing scheme, no roll-up is observed after the singularity, see figure 3, unlike in Kelvin–Helmholtz instability. A very accurate numerical method is required to observe the singularity. An open question is whether the smooth solution of equations (1.1), (1.2) modified by a surface-tension-like term is physically relevant for the long-term evolution, beyond the time at which the singularity spontaneously appears in the absence of the surface-tension-like term. The vortex produced by front wrinkling could become no longer negligible as soon as a strong increase of curvature develops locally, and a vortex sheet could appear in the hot fluid. If this were the case, the singularity would indicate a transition in the dynamics of the pattern, beyond which the present analysis would fail. This seems to be the case in the direct numerical simulation presented by Betti & Sanz (2006) who investigated the role of the vorticity for $\nu = 5/2$, $Fr^{-1} = 0.2$ and a real density profile. In this respect the influence of higher-order effects and the physical relevance of both the singularity and the limit of strong temperature dependence of thermal conductivity remain to be investigated.

This research was supported by the French program “Instabilités Hydrodynamiques intervenant en FCI en lien avec le LMJ” sponsored by the CEA-DIF and the CNRS. We would like to thank Professor Yves Pomeau for fruitful discussions and careful reading of the manuscript.

REFERENCES

- ATZENI, S. & MEYER-TER-VEHN, J. 2004 *The Physics of Inertial Fusion*, 1st edn. Oxford Science Publications.
- BAKER, G., CAFLISCH, R. E. & SIEGEL, M. 1993 Singularity formation during Rayleigh–Taylor instability. *J. Fluid Mech.* **252**, 51–78.
- BAKER, G. R., MEIRON, D. I. & ORSZAG, S. A. 1980 Vortex simulation of the Rayleigh–Taylor instability. *Phys. Fluids* **23**, 1485–1490.
- BETTI, R., GONCHAROV, V., MCCRORY, R. L. & VERDON, C. P. 1995 Self-consistent cutoff wave numbers of the Rayleigh–Taylor instability. *Phys. Plasmas* **2**, 3844–3851.
- BETTI, R., MCCRORY, R. L. & VERDON, C. P. 1993 Stability analysis of unsteady ablation fronts. *Phys. Rev. Lett.* **71**, 3131–3134.

- BETTI, R. & SANZ, J. 2006 Bubble acceleration in the ablative Rayleigh–Taylor instability. *Phys. Rev. Lett.* **97**, 205002.
- BODNER, S. 1974 Rayleigh–Taylor instability and laser-pellet fusion. *Phys. Rev. Lett.* **33**, 761–764.
- BYCHKOV, V., GOLBERG, S. M. & LIBERMAN, M. A. 1994 Self-consistent model of the Rayleigh–Taylor instability in ablatively accelerated laser plasma. *Phys. Plasmas* **1**, 2976–2986.
- CLAVIN, P. & ALMARCHA, C. 2005 Ablative Rayleigh–Taylor instability in the limit of an infinitely large density ratio. *C. R. Méc.* **333**, 379–388.
- CLAVIN, P. & MASSE, L. 2004 Instabilities of ablations fronts in inertial fusion: a comparison with flames. *Phys. Plasmas* **11**, 690–705.
- CLAVIN, P. & WILLIAMS, F. 2005 Asymptotic spike evolution in Rayleigh–Taylor instability. *J. Fluid Mech.* **525**, 105–113.
- DUCHEMIN, L., JOSSEAND, C. & CLAVIN, P. 2005 Asymptotic behavior of the Rayleigh–Taylor instability. *Phys. Rev. Lett.* **94**, 224501.
- GONCHAROV, V., BETTI, R., MCCRORY, R. L., SOROTOKIN, P. & VERDON, C. P. 1996 Self-consistent stability analysis of ablation fronts with large Froude numbers. *Phys. Plasmas* **3**, 1402–1414.
- LAYZER, D. 1955 On the instability of superimposed fluids in a gravitational field. *Astrophys. J.* **122**, 1–12.
- MATSUOKA, C. & NISHIHARA, K. 2006 Erratum: Vortex core dynamics and singularity formations in incompressible Richtmyer–Meshkov instability. *Phys. Rev. E* **73**, 026304 (2006). *Phys. Rev. E* **74**, 049902.
- MOORE, D. W. 1979 The spontaneous appearance of a singularity in the shape of evolving vortex sheet. *Proc. R. Soc. Lond. A* **365**, 105–119.
- PELCÉ, P. & CLAVIN, P. 1982 Influence of hydrodynamics and diffusion upon the stability limits of laminar premixed flames. *J. Fluid Mech.* **124**, 219–237.
- PIRIZ, A. 2001 Hydrodynamic instability of ablation fronts in inertial confinement fusion. *Phys. Plasmas* **8**, 997–1002.
- PIRIZ, A. R., SANZ, J. & IBAÑEZ, L. F. 1997 Rayleigh–Taylor instability of the steady ablation fronts: The discontinuity model revisited. *Phys. Plasmas* **4**, 1117–1126.
- SANZ, J. 1994 Self-consistent analytical model of the Rayleigh–Taylor instability in inertial confinement fusion. *Phys. Rev. Lett.* **73**, 2700–2703.
- SANZ, J. 1996 Self-consistent analytical model of the Rayleigh–Taylor instability in inertial confinement fusion. *Phys. Rev. E* **53**, 4026–4045.
- SANZ, J., MASSE, L. & CLAVIN, P. 2006 The linear Darrieus–Landau and Rayleigh–Taylor instabilities in inertial confinement fusion revisited. *Phys. Plasmas* **13**, 102702.
- SANZ, J., RAMÍREZ, J., RAMIS, R., BETTI, R. & TOWN, R. P. J. 2002 Nonlinear theory of the ablative Rayleigh–Taylor instability. *Phys. Rev. Lett.* **89**, 195002.
- TAYLOR, G. I. 1950 The instability of liquid surfaces when accelerated in a direction perpendicular to their plan. *Proc. R. Soc. Lond.* **201**, 192–196.